Electron. Mater. Lett., Vol. 10, No. 1 (2014), pp. 101-106
DOI: 10.1007/s13391-013-3168-1

Effect of Te on Linear and Non-linear Optical Properties of New Quaternary Ge-Se-Sb-Te Chalcogenide Glasses

Neha Sharma,[1] Sunanda Sharda,[1] S.C. Katyal,[2] Vineet Sharma,[1] and Pankaj Sharma[1,*]

[1]Department of Physics and Materials Science, Jaypee University of Information Technology, Waknaghat, Solan, H.P. (173234), India
[2]Department of Physics, Jaypee Institute of Information Technology, Sec - 128, Noida, UP, 201301, India

(received date: 8 June 2013 / accepted date: 2 July 2013 / published date: 10 January 2014)

We report linear and non-linear optical properties of a new quaternary chalcogenide glass series $Ge_{19-y}Se_{63.8}Sb_{17.2}Te_y$ (y = 0, 2, 4, 6, 8, 10). In linear optical properties; refractive index, extinction coefficient and the Tauc gap are reported and their variation with Te content has been discussed. In non-linear properties; third order non-linear susceptibility and non-linear refractive index has been discussed. The variation of non-linear refractive index has also been reported with normalized photon energy. A correlation between the Tauc gap and non-linear refractive index has been discussed. Results indicate that these materials may find applications in modern optical devices.

Keywords: optical materials, thin films, tauc gap, refractive index

1. INTRODUCTION

Chalcogenide glasses are truly remarkable optical materials due to their high linear and non-linear refractive index[1] and photoinduced phenomena (*i.e.* from photodarkening to photocrystallization).[2] Glasses prepared from heavy chalcogen (Te) offer huge benefit for developing materials that show transparency in Far-infrared region.[3] Glasses have strong polarizability of bonds due to which refractive index is high. Large refractive index leads to a large non-linear index due to which chalcogenide glasses have gained much interest in the field of non-linearity. Non-linear refractive index values of chalcogenide glasses are found to be several orders higher than conventional silica glasses at 1.55 μm.[1,4] Non-linear optical phenomena are suitable for all-optical processing functions and may be explored in future high-speed and high-capacity optical communication networks.[5] Non-linear signal processing has been used in various media such as optical fiber with low transmission loss, semiconductor optical amplifiers, etc.[5] Highly non-linear fibers can be used in various applications *viz.* supercontinuum generation, frequency metrology and wavelength conversion.[6]

Ge-Se-Sb glasses have low transmission loss and high transparency in infrared (IR) region from 2 - 14 μm which makes them suitable in optical fibers.[7] Physical, structural, thermal and optical properties have been carried out for $Ge_{19}Se_{81-x}Sb_x$ (y = 0, 4, 8, 12, 16, 17.2, 20) system.[8-11] Results indicate that ternary glasses with 19 at. % of Ge, has the highest T_g at an Sb content of x = 17.2 at. % consistent with the network backbone being fully polymerized.[8,9,12,13] Two intrinsic factors restricting the transparency of glasses in UV-visible and infrared region. (i) Electronic absorption that affects the transparency in UV-visible region. (ii) Phonon absorption (due to vibrational modes) which occurs in infrared region.[3] Te has low phonon energy due to its high atomic weight and has transparency up to 25 μm.[14] Therefore, Te-based glasses find applications at longer wavelength in IR region such as CO_2 infrared sensing at 15 μm and outer space life detection.[14] Te based glasses are suitable for integrated optics and optical storage due to high refractive index, photosensitivity and rapid amorphous-to-crystalline transformation.[15-17]

In present work, we report the synthesis and effect of Te on Ge-Se-Sb system to study linear and non-linear optical properties. Addition of Te to $Ge_{19}Se_{63.8}Sb_{17.2}$ may be used in non-linear devices due to its band gap which is very close to the band gap suitable for optical devices.

2. EXPERIMENTAL PROCEDURE

Melt quench technique has been used for preparation of $Ge_{19-y}Se_{63.8}Sb_{17.2}Te_y$ (y = 0, 2, 4, 6, 8, 10) alloys. The materials were weighed according to their at. wt. % and sealed in evacuated (~10^{-4} Pa) quartz ampoules with each composition having 1 g batch. The sealed ampoules were kept inside a furnace, where the temperature was increased upto 1000°C at a heating rate of 3 - 4°C min^{-1}. The

*Corresponding author: pankaj.sharma@juit.ac.in

ampoules were frequently rocked for 24 hours at highest temperature to make the melt homogeneous. The quenching was done in ice cold water. Films of $Ge_{19-y}Se_{63.8}Sb_{17.2}Te_y$ composition were deposited on well cleaned microscopic glass substrates using vacuum thermal evaporation technique at a background pressure of ~10^{-4} Pa (Hindhivac Model No. 12A4D). Evaporation rate used for film deposition is 12 Ås^{-1}. Film thickness of the deposited films measured with DTM - 101 is 600 nm ± 25 nm. Films were kept inside the deposition chamber for 24 hours to achieve thermal equilibrium.[18] The compositions of evaporated samples have been measured by electron microprobe analysis (JEOL 8600 MX) on different spots with size (~2 μm). For the composition analysis, the constituent elements (Ge, Se, Sb and Te) and the quenched samples were taken as reference samples. The composition of 2 × 2 cm^2 thin film sample has been found to be uniform within the measurement accuracy of about ±1.5%. X-ray diffraction spectra of bulk in power mode and thin films in grazing angle mode were obtained from x-ray diffractometer (X'Pert Pro). The transmission spectra of the thin films were obtained using a double beam UV-Vis-NIR spectrophotometer (Perkin Elmer Lambda - 750). The slit width was kept at 1 nm and all the measurements were performed at room temperature (300 K).

3. RESULTS AND DISCUSSION

Amorphous nature of bulk and thin films of samples has been confirmed from x-ray diffraction spectra as no distinguishable peaks are observed (not shown here). Transmission spectra of $Ge_{19-y}Se_{63.8}Sb_{17.2}Te_y$ (y = 0, 2, 4, 6, 8, 10) thin films in Fig. 1 show a red shift in interference free region of spectra with increasing Te addition.

3.1 Refractive index and extinction coefficient

Refractive index (n), thickness (t_{correc}) and extinction coefficient (k) have been calculated using envelope method.[19,20] Calculated values of thickness have been listed in Table 1. Spectral distribution of n is shown in Fig. 2 and inset shows the variation of k with wavelength. Refractive index shows normal dispersion behavior and both n and k increase with increasing content of Te. The increase in refractive index is explained on the basis of increasing polarizability of atoms.

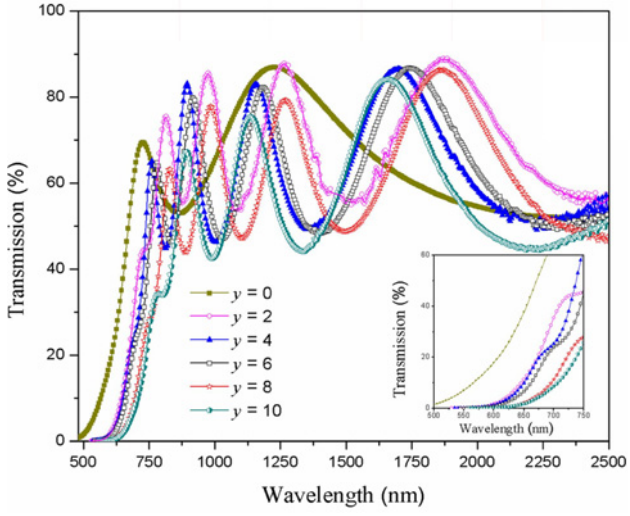

Fig. 1. Transmission spectra for $Ge_{19-y}Se_{63.8}Sb_{17.2}Te_y$ (y = 0, 2, 4, 6, 8, 10) thin films.

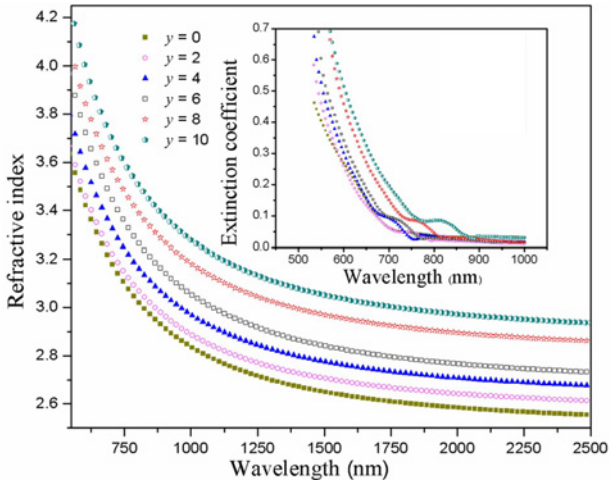

Fig. 2. Variation of refractive index (n) with wavelength (λ) for $Ge_{19-y}Se_{63.8}Sb_{17.2}Te_y$ (y = 0, 2, 4, 6, 8, 10). Inset shows the variation of extinction coefficient (k) with λ.

Table 1. Values of thickness (t_{correc}), dispersion energy (E_d), average energy gap (E_0), static refractive index (n_0), Tauc gap (E_g), lattice dielectric constant (ε_L), ratio of carrier concentration of effective mass (N/m^*), density of polarizable constituents (N'), non-linear refractive index (n_2),[36] n_2 at 1.55 eV[37] for $Ge_{19-y}Se_{63.8}Sb_{17.2}Te_y$ (y = 0, 2, 4, 6, 8, 10) thin films.

y	t_{correc} (nm)	E_d ± 0.01 (eV)	E_o ± 0.01 (eV)	n_o	Tauc gap (eV)	ε_L	$N/m^* \times 10^{56}$ ($m^{-3}kg^{-1}$)	$N' \times 10^{22}$ (cm^{-3})	$n_2 \times 10^{-10}$ (esu)[36]	$n_2 \times 10^{-09}$ (esu) at 1.55 eV [37]
0	227	21.88	3.41	2.72	1.57	7.7	4.66	3.69	1.59	1.07
2	662	20.07	3.17	2.71	1.55	8.12	5.89	3.66	1.54	1.23
4	593	21.05	3.13	2.78	1.52	8.63	6.14	3.62	1.90	1.53
6	596	21.66	3.06	2.84	1.51	9.13	7.98	3.59	2.26	1.93
8	617	23.42	3.05	2.95	1.46	9.64	8.34	3.56	3.07	2.52
10	538	25.30	3.04	3.05	1.42	10.17	9.87	3.53	4.01	3.21

Polarizability and refractive index are linked by Lorentz-Lorentz relation:[21]

$$\frac{n^2-1}{n^2+2} = \frac{1}{3\varepsilon_0}\sum_j N_j\alpha_{p,j} \quad (1)$$

where ε_0 is vacuum permittivity, N_j the number of polarizable units of type j per unit volume, with polarizability $\alpha_{p,j}$. Replacement of Ge (being less polarizable having atomic radius 1.22 Å) with Te (highly polarizable having 1.37 Å atomic radius) leads to an increase in refractive index of the system.[22] High value of refractive index has an advantage in strong optical field confinement that leads to the formation of compact circuit designs.[23] Increase in value of k with addition of Te content shows that loss of light increases due to scattering. Large value of k leads to high non-linear optical properties of the material. From the Kramer-Kronig relation, it is clear that red shift occur with increased refractive index value.[24]

The dispersion of refractive index has been analyzed in terms of WDD model which is based on single oscillator formula[25,26]

$$n^2-1 = \frac{E_dE_o}{E_o^2-(h\nu)^2} \quad (2)$$

where E_0 is single oscillator energy or average energy gap and E_d is dispersion energy and $h\nu$ is the photon energy. Factor E_d depends on the imaginary part of dielectric constant (ε_i) whereas E_0 does not. Due to this reason E_d is very nearly independent of E_o. Oscillator parameters calculated from the linear fit of $(n^2-1)^{-1}$ and $(h\nu)^2$ (Fig. 3) are given in Table 1. The dispersion plays a significant role with respect to optical communication and spectral dispersion.[27] The values of static refractive index (n_o) (Table 1) have been

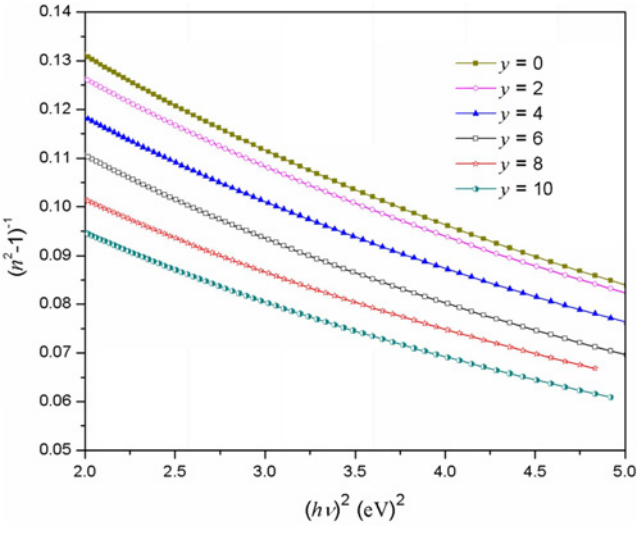

Fig. 3. Plot of $(n^2-1)^{-1}$ with $(h\nu)^2$ for $Ge_{19-y}Se_{63.8}Sb_{17.2}Te_y$ (y = 0, 2, 4, 6, 8, 10) thin films.

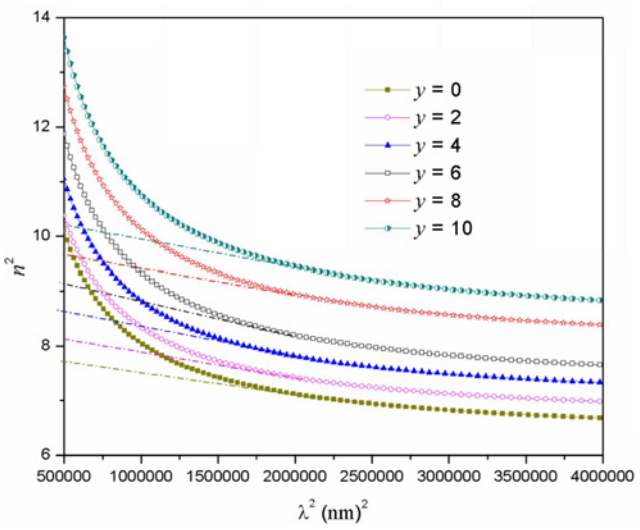

Fig. 4. Variation of n^2 with λ^2 for $Ge_{19-y}Se_{63.8}Sb_{17.2}Te_y$ (y = 0, 2, 4, 6, 8, 10) thin films.

calculated by extrapolating the WDD dispersion equation for $h\nu \to 0$. E_0 is related to the bond energy of chemical bonds present in system. When Ge is substituted with Te, high bond energy Ge-Se, Se-Te, Sb-Se and unsaturated Se-Se bonds are formed in respective order. Far-infrared study has also revealed the formation of Te-Te bonds.[10] With increasing Te content, probability of formation of Ge-Se bonds decreases while that of Se-Te and homopolar bond increases. Therefore, bond energy of the system decreases and hence values of E_o have been found to decrease.

Lattice dielectric constant ε_L and contribution of charge carriers (N) can be calculated from the relation:[28]

$$n^2 = \varepsilon_L - \left(\frac{e^2}{4\pi^2\varepsilon_o c^2}\right)\left(\frac{N}{m^*}\right)\lambda^2 \quad (3)$$

where e is charge of electron, (N/m^*) is the ratio of carrier concentration to effective mass and c is the velocity of light. Figure 4 show that n^2 is linearly dependent on λ^2 at longer wavelength. ε_L and (N/m^*) have been calculated by extrapolating plot to $\lambda^2 = 0$ and found to increase with increasing Te content (Table 1). According to Penn's theory,[29] $n^2 = 1 + (h\omega_p/E_g)^2$ where ω_p is plasma frequency and is determined using; $\omega_p^2 = 4\pi e^2 N/m^*$. With an increase in carrier concentration of charged states, Tauc gap (E_g) decreases and hence, refractive index increases.[30]

3.2 Absorption coefficient and Tauc gap

The absorption coefficient (α) for thin films has been calculated using relation:[19,20]

$$\alpha = \left(\frac{1}{d}\right)\ln\left(\frac{1}{X}\right) \quad (4)$$

where X is absorbance and d is thickness of the films. Inset

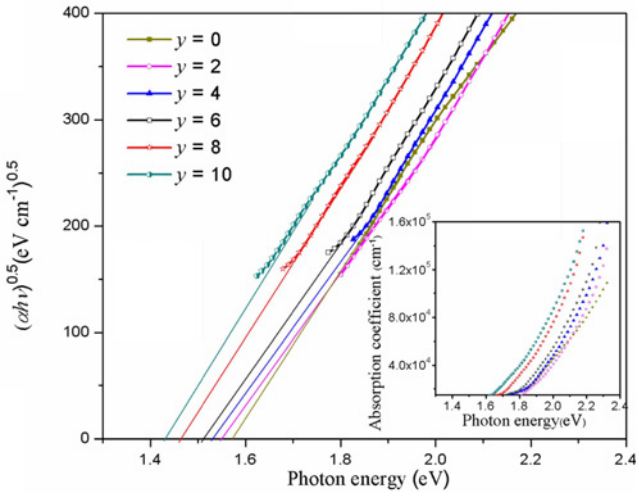

Fig. 5. Variation of $(\alpha h\nu)^{0.5}$ with photon energy ($h\nu$) and inset shows the absorption coefficient variation (α) with photon energy ($h\nu$) for $Ge_{19-y}Se_{63.8}Sb_{17.2}Te_y$ (y = 0, 2, 4, 6, 8, 10) thin films.

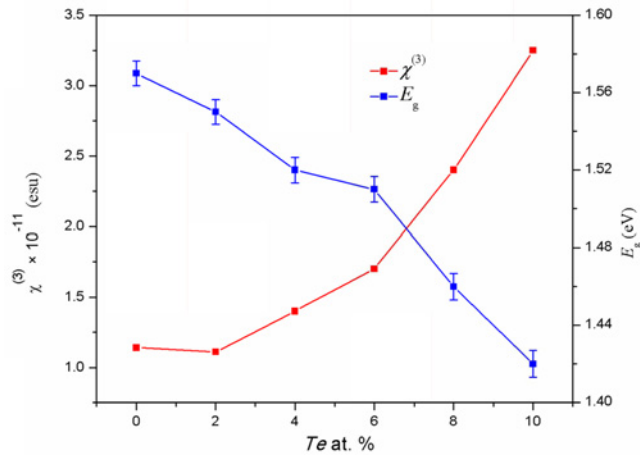

Fig. 6. Third order non-linear susceptibility ($\chi^{(3)}$) and E_g variation with Te content for $Ge_{19-y}Se_{63.8}Sb_{17.2}Te_y$ (y = 0, 2, 4, 6, 8, 10) thin films.

of Figure 5 shows that α increases with increasing energy and Te content. The Tauc gap has been calculated using relation:[31]

$$(\alpha h\nu)^{0.5} = B(\eta\nu - E_g). \quad (5)$$

B is energy tailing parameter that depends upon the width of localized states in the band gap. The relation $(\alpha h\nu)^{0.5} = f(h\nu)$ plotted in Fig. 5 shows the non-linear nature for all compositions indicating indirect allowed transition. The value of E_g can be estimated by the intercept of the extrapolations to zero absorption with the photon energy axis $(\alpha h\nu)^{0.5} \rightarrow 0$. Tauc gap has been found to decrease with increasing Te content (Table 1). Tauc gap of ternary system also decreases from 1.96 eV to 1.57 eV for $Ge_{19}Se_{81}$ to $Ge_{19}Se_{63.8}Sb_{17.2}$, after then increases for $Ge_{19}Se_{61}Sb_{20}$. Jhin *et al.* reported the Tauc gap having value 2.05 eV is comparable to 1.96 eV obtained in $Ge_{19}Se_{81}$ film.[32]

Average energy gap is related to Tauc gap by Tanaka's relation $E_0 \approx 2 \times E_g$.[33] The values obtained by Tanaka's relation are in agreement with those obtained from Tauc's relation. The number of states in conduction band depends upon the number of bonds and in valence band are due to the presence of lone pairs.[34] Te has a tendency to make defect states (D^0, D^+, D^-) and create chemical disordering in the system due to the presence of lone pair which increase with Te addition.[34] The decrease in E_g may be due to increase in density of localized states near the conduction band edge with incorporation of Te content.

3.3 Non-linear refractive index

When light of high intensity propagates through the medium, it causes non-linear effects. The non-linear refractive index in chalcogenide glasses is highly dependent on incident intensity. When matter is exposed to intense electric field of incident light, polarization is no longer proportional to electric field and the change in polarizability has to be extended by terms proportional to square of electric field.[35] n_2 has been calculated using two methods; (a) Tichy and Ticha[36] (b) Fournier and Snitzer.[37]

(a) Tichy and Ticha relation

This relation is a combination of Miller's generalized rule and static refractive index obtained from WDD model as:[36]

$$n_2 = \frac{12\pi\chi^{(3)}}{n_0} \quad (6)$$

where $\chi^{(3)}$ is third order non-linear susceptibility. $\chi^{(3)}$ is obtained from the relation; $\chi^{(3)} = A(\chi^{(1)})^4$,[38] where $\chi^{(1)}$ is linear susceptibility and is given as $\chi^{(1)} = \frac{E_d/E_0}{4\pi}$ and $A = 1.7 \times 10^{-10}$[36] (when χ is measured in esu). $\chi^{(3)}$ is given as:

$$\chi^{(3)} = \frac{A}{(4\pi)^4}(n_0^2 - 1)^4. \quad (7)$$

In general, band gap and polarizability are the key parameters to obtain high susceptibility. When Te is incorporated to GeSeSb composition, $\chi^{(3)}$ increases while E_g decreases as illustrated in Fig. 6. The values of n_2 for the investigated samples also show similar behavior (Table 1).

(b) Fournier and Snitzer

Fournier and Snitzer proposed a formula to determine the non-linear refractive index using linear refractive index and WDD parameters (E_o, E_d) in following relation:[37]

$$n_2 = \frac{(n^2+2)^2(n^2-1)E_d}{48\pi n N'(E_o)^2} \quad (8)$$

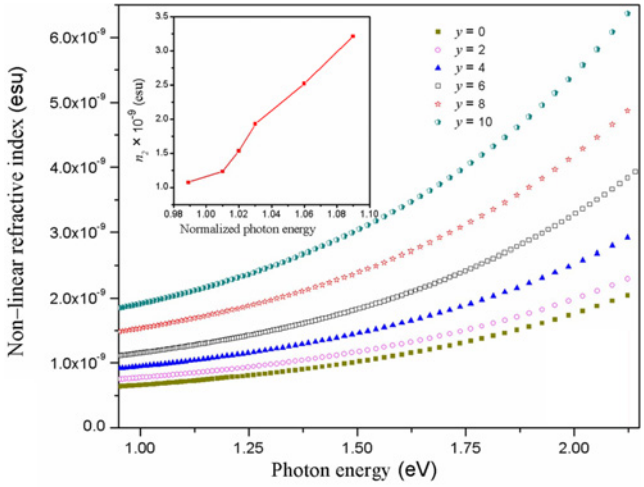

Fig. 7. Plot of non-linear refractive index (n_2) with photon energy ($h\nu$) for $Ge_{19-y}Se_{63.8}Sb_{17.2}Te_y$ ($y = 0$, 2, 4, 6, 8, 10) thin films. Inset shows the variation of n_2 with normalized photon energy ($h\nu/E_g$).

where N' is density of polarizable constituents. The calculated values of n_2 at 1.55 eV are listed in Table 1. Figure 7 show that n_2 increases with increase in photon energy and also with Te content.

Non-linearity of glasses can be explained on the basis of Tauc gap and defect states.[1,6] According to Moss rule, non-linearity can be determined from Tauc gap values as $n_2 \propto 1/(Eg)^4$.[39] With the increasing Te content, E_g^{opt} decreases and hence n_2 increases. Due to the presence of heteropolar and homopolar bonds, the probability of variety of defects gap states increase and this leads to an increase in non-linearity with the increase of Te content.[1,6] Increase in n_2 has also been confirmed from Far-infrared studies that indicate the presence of $GeSe_4$ (ν_2 mode), Se_6Te_2 rings, $GeTe_4$ tetrahedron, and Te-Te structural units.[10] Inset of Figure 7 shows that n_2 increases with increasing normalized photon energy ($h\nu/E_g$).[1]

Comparison of non-linear refractive index of investigated glasses with other materials at 1.55 eV shows that n_2 for; pure silica is 7.4×10^{-14},[40] $Ge_{10}As_{30}Se_{60}$ is 7.33×10^{-11},[36] $Ge_{10}Sb_{30}Se_{60}$ is 1.1×10^{-10},[36] $(As_2Se_3)_{90}Ge_{10}$ is 2.94×10^{-11}[35] and $[(As_2Se_3)_{90}Ge_{10}]_{95}Bi_5$ is 7.06×10^{-11}.[35] The values of n_2 for $Ge_{19-y}Se_{63.8}Sb_{17.2}Te_y$ ($y = 0$, 2, 4, 6, 8, 10) chalcogenide glasses are higher than these glasses. Our investigated glasses have large non-linear values that may be used in the formation of small, compact and low power devices for telecommunication applications.

4. CONCLUSIONS

Transmission spectra of evaporated $Ge_{19-y}Se_{63.8}Sb_{17.2}Te_y$ ($0 < y < 10\%$) thin-films show the optical band gap to steadily red shift in the $1.57 < E_g < 1.42$ range with increasing Te content. Non-linear refractive index has been observed to increase with increasing Te content. An increasing value of non-linear refractive index with Te depends upon the E_g and the presence of different bonds formed. These chalcogenide glasses exhibit high linear and non-linear refractive index which makes them potential candidates for integrated optics, ultrahigh-bandwidth signal processing and infrared optical sensors for medical applications.

REFERENCES

1. L. Petit, N. Carlie, H. Chen, S. Gaylord, J. Massera, G. Boudebs, J. Hu, A. Agarwal, L. Kimerling, and K. Richardson, *J. Solid State Chem*. **182**, 2756 (2009).
2. Y. Gueguen, J. C. Sangleboeuf, V. Keryvin, E. Lepine, Z. Yang, T. Rouxel, C. Point, B. Bureau, X.-H. Zhang, and P. Lucas, *Phys. Rev. B* **82**, 134114 (2010).
3. B. Bureau, C. Boussard-Pledel, P. Lucas, X. H. Zang, and J. Lucas, *Molecules* **14**, 4337 (2009).
4. R. R. Rojoa, T. Kosa, E. Hajto, P. J. S. Ewen, A. E. Owen, A. K. Kar, and B. S. Wherrett, *Opt. Commun*. **109**, 145 (1994).
5. M. D. Pelusi, V. G. Taeed, L. Fu, E. Magi, M. R. E. Lamont, S. Madden, D. Y. Choi, D. A. P. Bulla, B. Luther-Davis, and B. J. Eggleton, *IEEE J. Sel. Top. Quantum Electron*. **14**, 529 (2008).
6. J. T. Gopinath, M. Soljacic, and E. P. Ippen, *J. Appl. Phys*. **96**, 6931 (2004).
7. P. Sharma, V. S. Rangra, P. Sharma, and S. C. Katyal, *J. Alloy. Compd*. **480**, 934 (2009).
8. N. Sharma, S. Sharda, V. Sharma, and P. Sharma, *Defect and Diffusion Forum* **316-317**, 37 (2011).
9. N. Sharma, S. Sharda, V. Sharma, and P. Sharma, *Mat. Chem. Phys*. **13**, 967 (2012).
10. N. Sharma, S. Sharda, V. Sharma, and P. Sharma, *J. Non-Cryst. Solids* **375**, 114 (2013).
11. N. Sharma, S. Sharda, V. Sharma, and P. Sharma, *J. Non-Cryst. Solids* **371-372**, 1 (2013).
12. S. Mahadevan and A. Giridhar, *J. Non-Cryst. Solids* **143**, 52 (1992).
13. P. Boolchand, D. G. Georgiev, T. Qu, F. Wang, L. Chai, and S. Chakravarty, *C. R. Chim*. **5**, 713 (2002).
14. J. Sun, Q. Nie, X. Wang, S. Dai, X. Zhang, B. Bureau, C. Boussard, C. Conseil, and H. Ma, *Infrared Phys. Technol*. **55**, 316 (2012).
15. V. Pamukchieva, A. Szekeres, K. Todorova, M. Fabian, E. Svab, Z. Revay, and L. Szentmiklosi, *J. Non-Cryst. Solids* **355**, 2485 (2009).
16. J. Akola and R. O. Jones, *Phys. Rev. B* **76**, 235201 (2007).
17. J. Akola and R. O. Jones, *Phys. Rev. Lett*. **100**, 205502 (2008).
18. M. Abkowitz, G. M. T. Foley, J. M. Markovics, and A. C. Pulumbo, *AIP Conf. Proceedings*, **120**, 117 (1984).
19. R. Swanepoel, *J. Phys. E: Sci. Instrum*. **16**, 1214 (1983).

20. R. Swanepoel, *J. Phys. E: Sci. Instrum*. **17**, 896 (1984).
21. J. M. Gonzalez-Leal, R. Prieto-Alcon, J. A. Angel, and E. Marquez, *J. Non-Crys. Solids* **315**, 134 (2003).
22. C. N. R. Rao, M. V. George, J. Mahanty, and P. T. Narasimhan, *Handbook of Chemistry and Physics*, p. 209, Affiliated East-West Press, New Delhi, 1970.
23. V. G. Taeed, N. J. Baker, L. Fu, K. Finsterbusch, M. R. E. Lamonti, D. J. Moss, H. C. Nguyen, B. J. Eggleton, D. Y. Choi, S. Madden, and B. Luther-Davis, *Opt. Express.* **15**, 9205 (2007).
24. E. Marquez, J. M. Gonzalez-Leal, A. M. Bernal-Oliva, T. Wagner, and R. Jimenez-Garay, *J. Phys. D: Appl. Phys.* **40**, 5351 (2007).
25. S. H. Wemple and M. DiDomenico, *Phys. Rev. B* **3**, 1338 (1971).
26. S. H. Wemple, *Phys. Rev. B* **7**, 3767 (1973).
27. M. Fadel, S. A. Fayek, M. O. Abou-Helal, M. M. Ibrahim, and A. M. Shakra, *J. Alloy. Compd.* **485**, 604 (2009).
28. A. Dahshan, H. H Amer, and K. A. Aly, *J. Phys. D: Appl. Phys.* **41**, 215401 (2008).
29. D. Minkov, E. Vateva, E. Skordeva, D. Arsova, M. Nikiforova, and G. Nadjakov, *J. Non-Cryst. Solids* **90**, 481 (1987).
30. M. M. Abdel-Aziz, E. G. El-Metwally, M. Fadel, H. H. Labib, and M. A. Afifi, *Thin Solid Films* **386**, 99 (2001).
31. D. L. Wood and J. Tauc, *Phys. Rev. B* **5**, 3144 (1972).
32. M. Jin, P. Chen, P. Boolchand, T. Rajagopalan, K. L. Chopra, K. Starbova, and N. Starbov, *Phys. Rev. B* **78**, 21420 (2008).
33. K. Tanaka, *Thin Solid Films* **66**, 271 (1980).
34. V. Pamukchieva, A. Szekeres, K. Todorova, M. Fabian, and E. Svap, *Opt. Mat*er. **32**, 45 (2009).
35. P. Sharma and S. C. Katyal, *J. Appl. Phys.* **107**, 113527 (2010) .
36. H. Ticha and L. Tichy, *J. Optoelectron. Adv. Mat*er. **4**, 381 (2004).
37. J. Fournier and E. Snitzer, *IEEE J. Quantum Electron*. **10**, 473 (1974).
38. C. Wang, *Phys. Rev. B* **2**, 2045 (1970).
39. T. S. Moss, *Phys. Stat. Sol. (b)* **131**, 415 (1985).
40. A. Boskovic, S. V. Chemikov, J. R. Taylor, K. L. Gruner-Nielsen, and O. A. Levring, *Opt. Lett*. **21**, 1966 (1996).